Fluoride glasses based on the $ZrF_4 – BaF_2 – MnF_2$ system

T. DJOUAMA, A. BOUTARFAIA, M. POULAIN[a*]
Laboratoire de Chimie Appliquée, Université M. Khider, BP 145, RP-Biskra, Algérie
[a]*"Sciences Chimiques", Université Rennes1, Campus Beaulieu, F-35042 Rennes, France*

Glass formation has been studied in the ZrF_4-BaF_2-MnF_2 ternary system. Two different vitreous areas have been observed. One of them corresponds to high concentrations in manganese fluoride, which confirms the vitrifying ability of MnF_2. The stability of these glasses versus devitrification has been increased by the incorporation of AlF_3 and ZnF_2. Glass compositions and partial vitreous areas are reported in the ZrF_4-BaF_2-MnF_2-AlF_3-ZnF_2 system. The evolution of characteristic temperatures and density versus chemical composition has been studied. These glasses have a potential for phoinduced phenomena.

(Received February 8, 2007; accepted February 14, 2007)

Keywords: Fluoride glasses, Manganese fluoride, Glass transition, Devitrification, Density

1. Introduction

Heavy metal fluoride glasses (HMFG) have been the subject of numerous studies [1-4]. Various fluorides act as glass progenitors when they are associated with alkali fluorides or earth alkali fluorides. The fluorozirconate group has emerged as the main HMFG that could lead to commercial optical components: special devices and optical fibers have been developed for medical applications, instrumentation and sensing [5,6]. Transition metal fluorides have been identified as glass progenitors in the early stage of fluoride glass research [7], providing the basis for various fundamental studies. While colored glasses appear less attractive for optical transmission, zinc fluoride was largely used in multicomponent glasses. Since binary ZnF_2-SrF_2 glasses are observed, ternary glasses based on ZnF_2 have been investigated [8].

There are similarities between manganese difluoride MnF_2 and ZnF_2. In particular, a MnF_2-BaF_2 binary glass has been reported [4]. Fluoride glasses based on divalent cations exhibit a low phonon energy and should be transparent at longer wavelength in the IR spectrum. Limited data are available in this area, mainly because these glasses are prone to devitrification.

The aim of this paper is to enlarge the search for glasses containing a large amount of manganese, both for fundamental purpose – to collect data and to understand the mechanisms of glass formation – and for potential developments. The most attractive field of investigations concerns photoinduced phenomena that have attracted considerable attention in recent years, especially in chalcogenides and silica glass [9-12]. Divalent manganese shifts the UV-visible edge towards visible spectrum. As a consequence, visible lasers could induce effects that ussually occur with UV lasers. With 5 d electrons, Mn^{2+} ions are highly paramagnetic, which opens prospects for magneto-optic effects. Finaly, the photoinduced defects that lead to photodarkening relate to changes in oxidation state of elements. In this respect, manganese also offers exetnded possibilities.

The starting point of the experimental study is the (Mn,Ba) F_2 binary glass. This glass requires a fast cooling to avoid devitrification. Other fluorides are added to this binary combination to reduce crystallization rate at cooling. This approach is based on the empirical "confusion principle" that expresses that glass stability is likely to increase when the number of glass components increases. A set of synthesis has been implemented using zirconium fluoride, aluminium fluoride and zinc fluoride to enhance glass formation.

2. Experimental

Starting materials are anhydrous fluorides: BaF_2 from Acros, AlF_3 from Central Glass, ZnF_2 and NH_5F_2 from Riedel de Haën. Oxides are ZrO_2 from Criceram and MnO from Prolabo.

Manganese difluoride was prepared by the chemical action of aqueous hydrofluorhydric acid onto $MnCO_3$ (Merck Pro Analysis) followed by drying at 250 °C. It is also synthesized using the ammonium fluoride processing described below.

The density of samples was determined using a helium picnometer (Micromeritics, AccuPyc 1330). The chemical composition of glasses has been checked by element analysis using energy dispersion spectrometry (Oxford Link ISIS) set-up incorporated into a (ISM 6400 JEOL) scanning electron microscope.

Glasses were synthesized using the ammonium bifluoride processing [4.12]: the batch consisting in the mixture if the calculated amount of fluorides and oxides was set in a long platinum crucible with an excess of ammonium bifluoride, acting as a fluorinating reagent. Once the fluorination stage was completed, batch was heated up to melting and homogenized. For this purpose, melt was heated around 700 °C for 5 to 15 min. Then melt

was poured onto a brass plate and squeezed by an upper metal plate to ensure fast quenching. The estimated cooling rate is in the range 100 to 1000 K/s. Thin glass samples, 0.3 to 0.8 mm in thickness, are obtained in this way.

Fluorination stage is a critical step that depends on the oxides to be fluorinated. It includes several steps with the formation of ammonium complex fluorides. Global reactions may be written as:

$$ZrO_2 + 2\ NH_4F, HF \rightarrow ZrF_4 + 2\ NH_3 + 2\ H_2O$$
$$MnO + NH_4F, HF \rightarrow MnF_2 + NH_3 + H_2O$$

The real chemical reaction is more complex as it involves the intermediate formation of ammonium salts – e.g. $(NH_4)_3ZrF_7$ - that are decomposed at higher temperature. Consequently, the amount of ammonium hydrogenofluoride required for complete fluorination is much larger than the stoichiometric amount suggested by the above chemical equations. For transition metals, especially manganese, fluorination temperature must be kept lower to prevent hydrolysis and, as a result, fluorination time is longer.

The vitreous nature of the samples is checked by visual inspection and microscopic observation. X-ray diffraction always leads to an amorphous pattern when clear samples are obtained.

Characteristic temperatures are measured by Differential Scanning Calorimetry using a Seiko DSC 220 set-up. Samples are set in a sealed aluminum pan and heated under argon flow at a standard heating rate of 10 $K.s^{-1}$. Glass transition appears as a change in the base line, which corresponds to the Cp variation between the solid state and the liquid state. The value assigned to T_g is the temperature of the intercept of the tangent to the solid base line and the tangent at the inflexion point. Devitrification corresponds to one or several exothermic peaks when sample is in the liquid state, that is at temperature higher than T_g but lower than the liquidus temperature. It is usually characterized by T_x, the temperature for onset of crystallization and T_c, the temperature of the maximum of the exotherm. The estimated accuracy is 2 °C for T_g and T_x and 1 °C for T_c.

The stability of the glass versus devitrification could be accurately defined by the critical cooling rate (CCR) [13], for which the crystalline fraction of the glass is smaller than a given limit, usually 10^{-6}. In turn, this critical cooling rate rules the maximum sample thickness, which is of practical importance. While the experimental determination of the CCR is often difficult, the assessment of the glass stability can be determined from the values of the characteristic temperatures. A common stability criterion is the difference between glass transition and onset of crystallization [14] $\Delta T = T_x - T_g$. An other stability criterion is expressed by the S factor [15] defined as: $S = (T_p - T_x)(T_x - T_g) / T_g$.

3. Results

3.1 The ZrF_4-BaF_2-MnF_2 system

3.1.1 Glass formation

A first set of synthesis has been implemented in the $ZrF_4 – BaF_2 – MnF_2$ ternary system. The glass forming areas appear in Fig. 1. There are two vitreous areas, along the ZrF_4-BaF_2 binary and the MnF_2-BaF_2 binary respectively. This observation is consistent with the occurrence of binary glasses in both systems. The limits of these areas correspond to quenched glasses. They may be summarized as follows:

$$48 < ZrF_4 < 80$$
1st zone $\quad 18 < BaF_2 < 53$
$$0 < MnF_2 < 15$$

$$0 < ZrF_4 < 30$$
2nd zone $\quad 20 < BaF_2 < 45$
$$40 < MnF_2 < 70$$

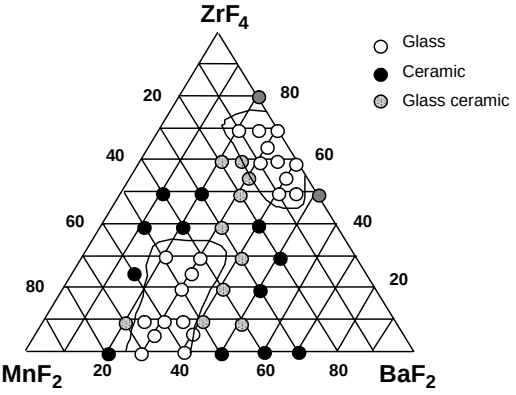

Fig. 1. Glass formation range (mol%) of the ZrF_4-BaF_2-MnF_2 system.

3.1.2 Thermal analysis

The characteristic temperatures and the stability criteria are reported in Table 1. It appears that glasses with high MnF_2 content exhibit a larger tendency to devitrification, as exemplified by the small value of the stability criteria. A typical DSC curve is shown in Fig. 2. The limited glass stability may be seen from the small difference between the respective temperatures for glass transition and crystallization. Also the sharp profile of the exotherm is often associated with fast devitrification kinetics.

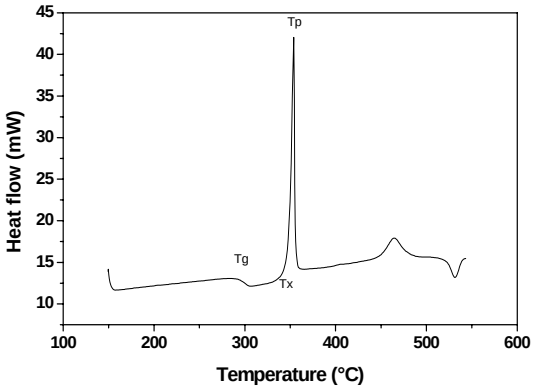

Fig. 2. DSC scan of the 30% ZrF_4 – 20% BaF_2 – 50% MnF_2 glass sample (ZBM 13).

Table 1. Characteristic temperatures of ZrF_4-BaF_2-MnF_2 glasses: T_g for glass transition, T_x for onset of crystallization and T_p for the maximum of the exotherm. S and T_x-T_g are stability criteria.

ZrF_4 %	BaF_2 %	MnF_2 %	Tg (°C)	Tx (°C)	Tp(°C)	Tx-Tg(°C)	S(K)	Acronym
60	35	5	300	356	368	56	1,26	ZBM1
65	30	5	300	342	354	42	0,88	ZBM2
55	40	5	314	361	374	47	1,09	ZBM6
60	36	4	299	347	363	48	1,35	ZBM5
75	20	5	293	328	335	35	0,43	ZBM9
50	40	10	315	367	378	52	0,96	ZBM12
55	30	15	299	342	351	43	0,66	ZBM15
30	30	40	299	351	357	52	0,47	ZBM14
20	30	50	299	322	328/407	23	0,23	ZBM7
5	40	55	330	352	358/368	22	0,22	ZBM3
30	20	50	290	347	354	56	0,73	ZBM13
10	30	60	297	313	316/370	16	0,07	ZBM8
0	30	70	377	395	418	18	0.63	ZBM0

3.2 The ZrF_4-BaF_2-MnF_2- AlF_3 –ZnF_2 system

3.2.1 Glass formation

In order to improve the quality of the glasses, aluminum fluoride and zinc fluoride have been added to the ternary components. These compounds were chosen because they are vitrifiers. A set of preparations were carried out with content in AlF_3 and ZnF_2 ranging from 5 to 20 mole %. Results are given either as a list of glass compositions (Table 2) or as pseudo ternary diagrams reported at Figs. 3a and 3b. The thermal characteristics of the first set of vitreous samples are reported in Table 2.

In a general way, these multicomponent glasses show a smaller devitrification tendency upon cooling, even though this is not always expressed by the values of the stability criteria.

Table 2. Characteristic temperatures and thermal stability range of the ZrF_4-BaF_2-MnF_2- AlF_3/ZnF_2 glasses.

ZrF_4 %	BaF_2 %	MnF_2 %	AlF_3 %	ZnF_2 %	T_g (°C)	T_x (°C)	T_p (°C)	T_x - T_g (°C)	S(K)	Acronym
45	25	10	15	15	314	376	388	62	1.27	T31
30	25	15	15	15	317	402	414	85	1.73	T27
25	35	20	10	10	311	354	356	43	0.15	T39
25	25	20	15	15	319	421	429	102	1.38	T26
40	30	25	5	0	319	384	392	65	0.88	T25
25	30	25	10	10	316	366	373	50	0.59	T24
20	25	25	15	15	317	406	414	89	1.21	T23
30	25	25	10	10	309	395	404	86	1.33	T1bis
25	25	30	0	20	284	337	346/358/405	53	0.86	T33
25	25	30	5	15	294	357	362	63	0.56	T19
20	30	30	10	10	309	355	360	46	0.40	T22
25	25	30	10	10	304	393	404	89	1.70	T22bis
25	25	30	15	5	320	412	425	92	2.02	T20
25	25	30	20	0	340	427	436	87	1.28	T32
15	25	30	15	15	318	395	402	80	0.91	T28
10	25	35	15	15	315	360	373	45	0.99	T29
25	25	35	0	15	287	344	351	57	0.71	T6
25	25	35	5	10	293	362	372	69	1.22	T3
25	25	35	10	5	312	395	406	83	1.56	T2
20	25	35	10	10	303	375	385	72	1.25	T1
25	20	35	10	10	300	375	386	75	1.44	T40
25	25	35	15	0	323	411	420	88	1.33	T5
10	30	40	10	10	312	359	365	47	0.48	T13
25	15	40	10	10	292	338	343/389	46	0.41	T38
15	25	40	15	5	321	383	391	62	0.84	T7bis
20	25	40	5	10	296	344	347	48	0.25	T9
20	30	40	5	5	295	334	338	39	0.27	T34
15	25	45	5	10	296	338	341	42	0.22	T10
20	20	45	8	7	300	378	386	78	1.09	T12
10	25	45	10	10	308	356	360	48	0.33	T14
20	25	45	5	5	296	341	348	45	0.55	T35
20	20	50	5	5	293	353	367	60	1.48	T17
10	25	50	10	5	306	353	357	47	0.32	T16
10	15	55	10	10	289	327	334/386	38	0.47	T18
20	15	55	5	5	282	332	338	50	0.54	T36
15	25	35	15	10	320	375	382	55	0.65	T4
25	25	25	10	15	302	392	404	90	1.88	T41

Fig. 4 depicts the DSC curve of the 20%ZrF_4-20%BaF_2-50%MnF_2-5%AlF3-5%ZnF_2 (T17) glass together with the curve of the 25%ZrF_4-25%BaF2-25%MnF_2-10%AlF_3-15%ZnF_2 (T40) glass. Glass transition temperature T_g occurs at 293 °C for T17 and 300 °C for T40 while onset of crystallisation T_x is observed at 353 °C and 375 °C, respectively.

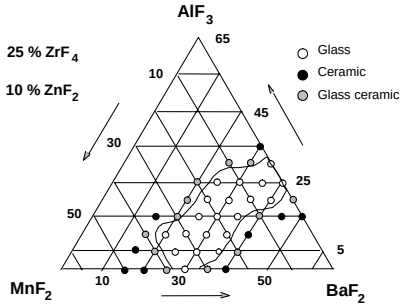

a

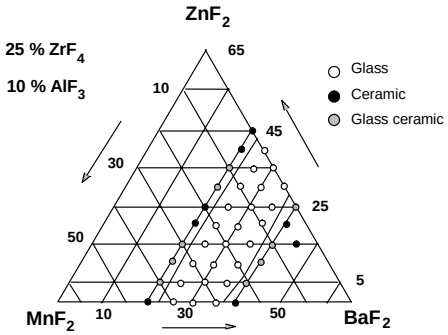

b

Fig. 3. Vitreous areas in the multicomponent systems 25%ZrF_4-BaF_2-MnF_2-AlF_3-10%ZnF_2 (a) and 25%ZrF_4-BaF_2-MnF_2-10%AlF_3-ZnF_2 (b).

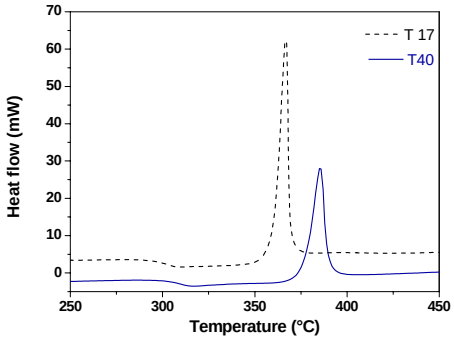

Fig. 4. DSC scan of the 20%ZrF_4-20%BaF_2-50%MnF_2-5%AlF_3-5%ZnF_2 (T17) and 25%ZrF_4-25%BaF_2-25%MnF_2-10%AlF_3-15%ZnF_2 (T40) glasses.

By comparison with the ternary glass (Fig. 2), the thermal stability range (T_x – T_g) is larger and the crystallisation exotherm is wider. Both features express the increased stability of the multicomponent glass samples.

3.2.2 Composition properties relations: ZnF_2 / AlF_3 substitution

Thermal properties are closely related to chemical composition. While it is difficult to assess the absolute contribution of each glass component, it is easier to compare two different additives, using a composition rule in which the other concentrations are kept constant. In a first step, a set of samples has been prepared with the general formula 25 ZrF_4 – 25 BaF_2 - 30 MnF_2 – x AlF_3- (20-x) ZnF_2. Fig. 5 shows the evolution of the glass transition temperature T_g, the thermal stability range and the density as a function of aluminium fluoride content. Not surprisingly, the general trend is that T_g increases while density decreases. Maximum stability range is observed around 10 % AlF_3.

3.2.3 Composition properties relations: MnF_2 / ZrF_4 substitution

A second set of samples correspond to (55 – x) ZrF_4 – 25 BaF_2 – x MnF_2 – 10 AlF_3 – 10 ZnF_2 glasses in which the ZrF_4/MnF_2 substitution is implemented. On the basis of the previous observation, these glasses contain 10 % AlF_3 to promote glass stability.

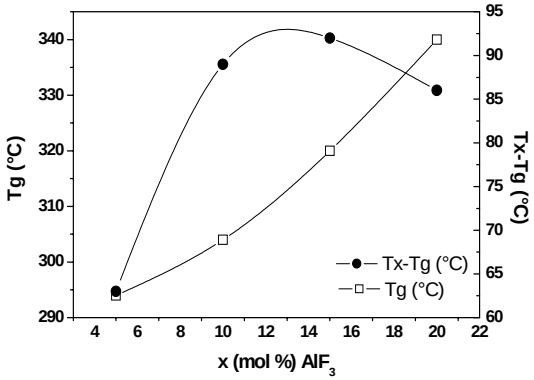

a

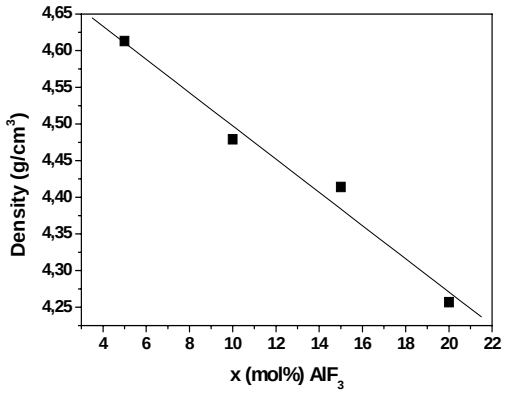

b

Fig. 5. Evolution of thermal characteristics (a); and density (b) versus x % AlF_3 in the 25% ZrF_4 - 25 % BaF_2 - 30% MnF_2 – x % AlF_3- (20-x) % ZnF_2 system.

Thermal characteristics and density evolution versus manganese content, are reported in Figs. 6a, 6b and 6c.

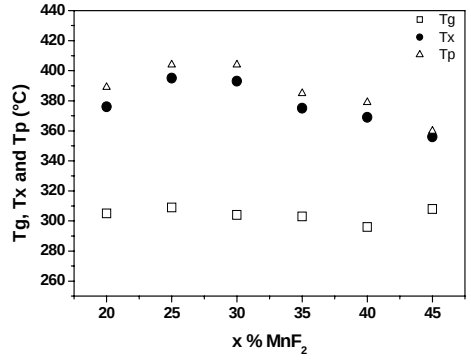

a

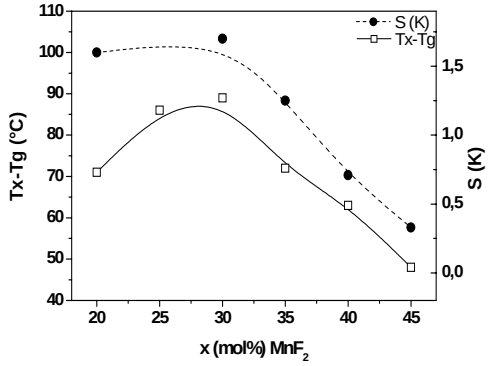

b

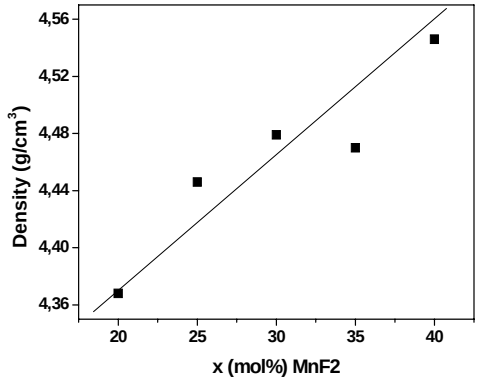

c

Fig. 6. Evolution of characteristic temperatures (a), stability criterion (T_x-T_g) and S(K) (b) and density (c) vs. MnF_2 content in (55-x)% ZrF_4-25% BaF_2-x%MnF_2-10%AlF_3-10%ZnF_2 system.

3.2.4 Composition properties relations: MnF_2 / AlF_3 substitution

Fig. 7 gathers the results corresponding to the AlF_3/MnF_2 substitution in the 25% ZrF_4-25% BaF_2-(35-x)% MnF_2- x% AlF_3- 15% ZnF_2 glasses.

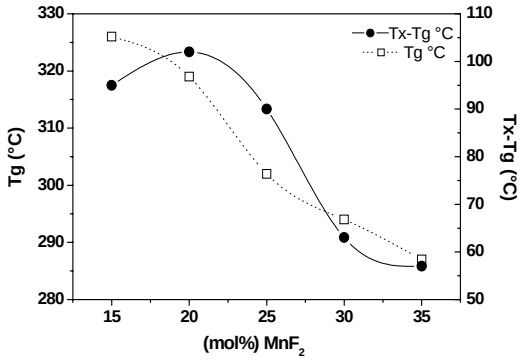

a

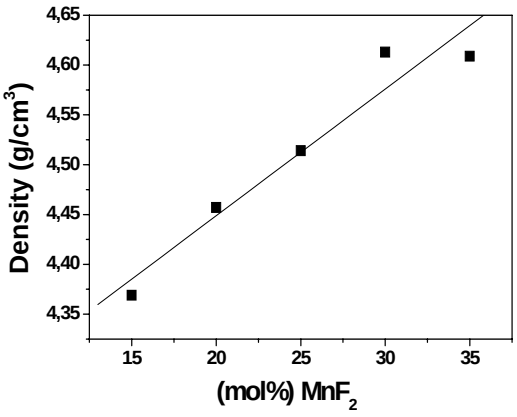

b

Fig. 7. Evolution of thermal characteristics (a) and density (b) versus % MnF_2 in the 25% ZrF_4 – 25 %BaF_2 – (35-x)% MnF_2 – x% AlF_3 –15% ZnF_2 system

3.2.5 Composition properties relations: MnF_2 / BaF_2 substitution

A similar set of samples have been prepared according to the composition rule 20% ZrF_4 –(70-x)% BaF_2 – x% MnF_2 – 5% AlF_3 –5% ZnF_2. As shown in Fig. 8, the T_g evolution is not monotonous while the thermal stability range is observed around 50 % MnF_2.

3.3 General properties

3.3.1 Optical transmission

By comparison to other heavy metal fluoride glasses [3.6], one could expect a wide transmission range in the mid-infrared. This is exemplified by Fig. 9 that shows a typical curve corresponding to a thin sample. Note that OH absorption around 3 micrometers is reduced.

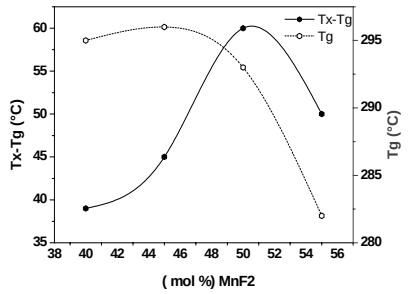

Fig. 8. Evolution of glass transition Tg and stability criterion Tx-Tg versus x % MnF_2 in the 20% ZrF_4 – (70-x) % BaF_2 – x % MnF_2 – 5% AlF_3 –5% ZnF_2 system.

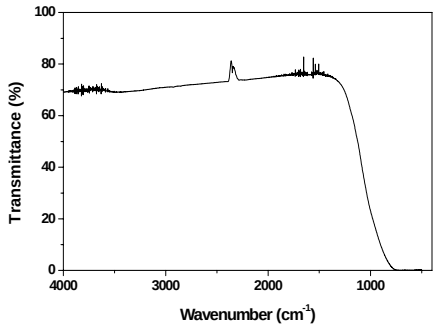

Fig. 9. Optical transmission range for the glass 25%ZrF_4 - 25%BaF_2 - 35%MnF_2 -5 %AlF_3 -10 %ZnF_2. Sample thickness: 0.8 mm.

3.3.2 Chemical durability

These glasses are stable at room atmosphere, even at high relative humidity. On the other hand, samples immersed in non-buffered liquid water at 25 °C show a surface attack after 15 hours, accompanied by the drop of the pH value. This behavior is similar to that of standard fluorozirconate glasses [23]. It does not seem that large MnF_2 content enhances the chemical durability.

4. Discussion

This study confirms that the $ZrF_4 – BaF_2$ binary glass may be stabilized by the limited addition (< 10 mol %) of one fluoride. The size of the vitreous area in the ternary system demonstrates that MnF_2 also has a stabilizing effect. However, the most attractive observation lies in the occurrence of manganese-rich glasses in the vicinity of the MnF_2-BaF_2 binary glass, which also confirms that MnF_2 may act as a glass progenitor. In this respect, there are similarities between zinc and manganese: both may form binary glasses and enter glass composition as major components. This experimental behavior is exemplified by Fig. 3b that shows that there is no change in the vitreous domain as MnF_2 substitutes ZnF_2. Then one may assume that manganese fluoride may be used in the same way as zinc fluoride to adjust physical properties of HMFG.

Glasses are currently described on the basis of the random network model [17] and it is usually assumed that glass forming ability is correlated to network stability. The crystal chemistry of the manganese fluoride complexes shows that they are constructed from MnF_6 octahedra [18] and this is also the conclusion of structural studies of MnF_2 containing glasses [19]. This suggests that the structure of the binary glasses consists in MnF_6 octahedra sharing corners and hosting large Ba^{++} cations. This simple picture should be confirmed by EXAFS and vibrational spectroscopy. The ease of the substitution ZnF_2/MnF_2 appears logical insofar as the ionic radii of the divalent cations are close - 74 pm and 83 pm respectively [20] - and both cations are octahedrally coordinated in fluorides. The incorporation of aluminium fluoride introduces additional flexibility because AlF_6 octahedra are smaller in size, and also it increases the average anion to cation ratio, which is expected to decrease the network connectivity. In glasses containing ZrF_4, the anion to cation ratio also increases with Zr content, but coordination polyhedra of Zr are larger. Mean coordination number of Zr is close to 8 [21], which corresponds to square antiprism – like in crystalline ZrF_4 [18] - or dodecahedron. This feature also increases the number of the possible configurations in network construction. Finally, the cations showing some stabilizing effect have a larger field strength than Mn^{2+}, which is consistent with the assumption that there must be an optimum balance between the average field strength of the cations, and that of the anions [22].

The two specific features of manganese-containing glasses are the shift of the UV- visible edge and the paramagnetic character of the Mn^{2+} ions. Early studies have confirmed that spin glasses may be obtained in this way [23]. The EPR hyperfine splitting pattern of Mn^{2+} ions in fluoride glasses provides limited structural information and confirms the ionic character of the Mn^{2+} environment [24]. There is also the possibility that they can modify optical properties under special conditions. Of special interest is the writing of optical waveguides [25,26] or Bragg gratings [27] and the control of photodarkening, using high power laser beams.

5. Conclusion

Vitreous areas have been investigated in the $ZrF_4 – BaF_2 – MnF_2$ ternary system and the occurrence of manganese rich glasses confirms the glass forming ability of the manganese difluoride. The incorporation of AlF_3 and ZnF_2 reduces devitrification tendency. The compositional dependence of the thermal properties and density has been studied by the implementation of the AlF_3/ZnF_2, MnF_2/ZrF_4, MnF_2/AlF_3 and MnF_2/BaF_2 substitutions. Glass transition temperature is close to 300 °C and the position of the infrared absorption edge is

consistent with early studies on HMFGs. These new glasses are attractive materials for magnetic and photosensitivity studies.

References

[1] M. Poulain, Heavy Metal Fluoride Glasses, in "Non crystalline Materials for Optoelectronics", M. Popescu ed, INOE publishing, Chapter **12**, 335-361 (2004).

[2] A. Comyns, "Fluoride Glasses", J. Wiley & Sons, Chichester, 219 (1989).

[3] I. Aggarwal, G. Lu, "Fluoride Glass Fiber Optics", Acad. Press, Boston, 401 (1991).

[4] M. Poulain, in: "Fluoride Glass Fiber Optics", Fluoride Glass Composition and Processing, ed. I. Aggarwal and G. Lu, Acad. Press., Boston 1 (1991).

[5] G. Mazé, in: "Fluoride Glasses", Applications and Prospects, ed. A. Comyns, J. Wiley & Sons, Chichester 201(1989).

[6] P. France, in: "Fluoride glass optical fibres", Applications", ed. P. W. France, Blackie, Glasgow (1990), p. 238

[7] J. P. Miranday, C. Jacoboni, R. De Pape, J. Non-Cryst. Solids **43**, 393 (1981).

[8] M. Poulain, Y. Messaddeq, Mat. Sci. Forum **32-33**, 131 (1988).

[9] M. Makyovanik, A. Kikineshi, S. H. Messaddeq, Y. Messaddeq, I. Yvan, S. J. L. Ribeiro, J. Non-Cryst. Solids **348**, 144-148 (2004).

[10] G. Brambilla, P. Hua, J. Non-Cryst. Solids **352**, 2921-2924 (2006).

[11] K. Czachor, K. Jedrzejewski, R. Stepien, Proc. SPIE. **5948**, 594819.1-594819.9 (2005).

[12] M. Poulain, G. Mazé, Chemtronics **3**, 77 (1988).

[13] M. C. Weinberg, D. R. Uhlmann, E. D. Zanotto, J. Am. Ceram. Soc.. **72**, 2054 (1989).

[14] A. Dietzel, Glastech. Ber. **22**, 41 (1968).

[15] M. Saad, M. Poulain, Mat. Sci. Forum **19-20**, 11 (1987).

[16] C. J. Simmons, J. Am. Ceram. Soc. **70**, 654 (1987).

[17] R. Zallen, "The Physics of Non-Cryst. Solids", J. Wiley & sons, New York, (1983).

[18] A. F. Wells, "Structural Inorganic Chemistry", Oxford University Press, Oxford, (1962).

[19] A. Le Bail, C. Jacoboni, R. De Pape, J. Solid State Chem. **52**, 32 (1984).

[20] R. D. Shannon, Acta Cryst **A32**, 751 (1976).

[21] R. Coupe, D. Louër, J. Lucas, A. J. Leonard, J. Am. Ceram. Soc. **66**, 523 (1983).

[22] M. Poulain, Nature **293**, 279 (1981).

[23] A. Le Bail, C. Jacoboni, R. De Pape, J. Solid State Chem. **48**, 168 (1983).

[24] J. O. Warne, J. R. Pilbrow, D. R. MacFarlane, J. Non-Cryst. Solids **140**, 314 (1992).

[25] H. Ebendorff-Heidepriem, Opt. Mater. **25**, 109-115 (2004).

[26] A. Streltsov, C. W. Ponader, J. F. Schroeder, Proc. SPIE **6261**, 626132.1-626132.6 (2006).

[27] S. A. Vassiliev, O. I. Medvekov, I. G. Korolev, A. S. Bozhkov, A. S. Kurkov, E. M. Dianov, Quantum Electron. Woodbury. **35**, 1085-1103 (2005).

*Corresponding author: marcel.poulain@univ-rennes1.fr